View metadata, citation and similar papers at core.ac.uk
brought to you by CORE
provided by TUT DPub

TAMPEREEN TEKNILLINEN YLIOPISTO
TAMPERE UNIVERSITY OF TECHNOLOGY

MIKKO PIRTTINIEMI

OPTIMIZATION OF A RECOVERY BOILER ECONOMIZER

Master's thesis work

Examiner: Professor Reijo Karvinen

TIIVISTELMÄ

MIKKO PIRTTINIEMI:
Tampereen teknillinen yliopisto
Diplomityö, 37 sivua, 2 liitesivua
Syyskuu 2016
Ympäristö- ja energiatekniikan DI-tutkinto-ohjelma
Pääaine: Energiatehokkuus
Tarkastaja: Reijo Karvinen

Avainsanat: esilämmitin, optimointi, lämmönsiirto, massa, Parveilualgoritmi

Tämän diplomityön tarkoitus on minimoida soodakattilan esilämmittimen massaa säilyttämällä lämmönsiirtokyky. Päätavoitteena on luoda uusi 1-dimensiollinen malli esilämmittimen lämmönsiirrolle ja käyttää muunneltua versiota Parveilualgoritmi -optimointimenetelmästä.

Esilämmittimen lämmönsiirron laskennassa suurimpina ongelmina ovat partikkelisäteilyn laskenta ja esilämmittimen pinnoille käytössä kertyvä alkalisuolokerrostuma. Lisäksi varsinaisessa optimoinnissa suurimpana ongelmana on esilämmittimen suunnittelumuuttujien lukumäärä, joka tekee optimoinnista ilman laskentatyökaluja lähes mahdotonta.

Diplomityön tuloksissa käydään läpi esilämmittimen kaikkien suunnittelumuuttujien yhtäaikainen optimointi, sekä yksittäisten suunnittelumuuttujien optimointi, mistä nähdään mahdolliset yleiset suunnat esilämmönsiirtimen toiminnan parantamiseksi. Lisänä käydään läpi virtauksen parametrien ja aineominaisuuksien vaikutusta kehitetyn lämmönsiirtomallin tuloksiin. Optimointiohjelmaan käydään läpi myös mahdollisia yksinkertaistuksia, jotka vähentävät optimointiin tarvittavaa laskenta-aikaa vaikuttamatta tuloksiin virherajojen ulkopuolella.

Diplomityön rahoittajana ja tehtävänkuvan antajana toimii Valmet Technologies Oy, joka myös antoi tarvittavat referenssitiedot ja geometrian ohjelman tulosten validoimiseksi.

ABSTRACT

MIKKO PIRTTINIEMI:
Tampere University of Technology
Master of Science Thesis, pages 37, Appendix pages 2
September 2016
Master's Degree Programme in Environmental and Energy Engineering
Major: Energy Performance
Examiner: Professor Reijo Karvinen

Keywords: economizer, optimization, heat transfer rate, mass, Particle Swarm Optimization

The aim of the present Master's Thesis is to minimize the mass of a recovery boiler economizer while retaining heat transfer rate. The study features building a new 1-dimensional heat transfer model for the case and optimizing the results by using a modified version of Particle Swarm Optimization method.

Economizer heat transfer calculation is problematic due to particle radiation and fouling induced by exhaust fumes from the boiler. Moreover, in terms of optimization, the number of design variables included in the optimization render the case next to impossible to solve without computational support.

Results feature optimization of full economizer geometry as well as individual design parameter study, where direct guidelines for dimensional changes are found. Effect of flow properties and parameters are studied as well as possible simplifications for the model in order to make the optimization less time consuming. The results are expected to lead into savings in material costs as well as reduced size and mass while retaining the functionality, or even increasing it.

The study was provided by Valmet Technologies Oy, which also provided the initial geometry and reference cases for validation of the model.

ACKNOWLEDGEMENTS

First I want to thank Professor Reijo Karvinen and Valmet Technologies Oy for providing me with this interesting project as well as providing me with support whenever I needed it. Professor Reijo Karvinen I especially want to thank for his keen interest and profound knowledge of heat transfer, fins and heat transfer machinery that provided me with motivation and tools for starting the project. Secondly, I want to thank Kaj Lampio, Antti Mikkonen, Turo Välikangas and Matti Lindstedt, whose knowledge and support towards the completion of the present Master's Thesis proved to be invaluable. Without their help, many crucial parts of the program building and model generation would have become higher obstacles, but because of their help were dealt with ease. Thirdly, I want to thank Jaakko Ormiskangas for all the brainstorming sessions that came up during the write-up of the program. Fourthly, special thanks to Jarmo Mansikkasalo from Valmet Technologies Oy for providing me with whatever information I needed for the project and for keeping in contact when necessary.

I also want to thank my family for financial and emotional support. My friends I want to thank for sharing their own experiences during their write-up of their Master's Theses making it possible to compare and relate my own process to what was being done by somebody else. Lastly, I want to thank my girlfriend Terhikki Kataja for her support, understanding and for taking my mind off from my project when needed.

CONTENTS

LIST OF FIGURES

NOMENCLATURE

CFD	Computational Fluid Dynamics
LMTD	Logarithmic Mean Temperature Difference
LMHTR	Log Mean Heat Transfer Rate
NTU	Number of Transfer Units
A	area
$A_{\text{pipefin},gas}$	gas total cross-area perpendicular to flow direction
A_{cavity}	cross-area of sootblowing cavity perpendicular to flow direction
c_1	optimization constant
c_2	optimization constant
c_p	specific heat capacity in constant pressure
d_{h}	hydraulic diameter
$d_{\text{h,pipefin}}$	hydraulic diameter of pipe-fin area
$d_{\text{h,cavity}}$	hydraulic diameter of sootblowing cavity
f	friction factor
h	convection coefficient
$h_{\text{p,eff}}$	effective heat flux coefficient
h_g	gas convection coefficient
h_w	water convection coefficient
k	conduction coefficient
k_{f}	fouling conduction coefficient
l_{fin}	fin length
l_p	pipe perimeter
L	economizer length
$\dot{m}$	mass flow
$\dot{m}_{\text{pipefin}}$	gas mass flow in pipe-fin area
$\dot{m}_{\text{cavity}}$	gas mass flow in sootblowing cavity
M	mass target function
Nu_{d}	Nusselt number
$\boldsymbol{p}$	vector of particle personal best results
P	perimeter
Pr	Prandtl number
$q_{\text{conduction}}$	one-dimensional conductive heat flux
$q_{\text{convection}}$	one-dimensional convective heat flux
$q_{\text{f,cond}}$	one-dimensional conductive heat flux in fouling layer
$q_{\text{fin,cond}}$	one-dimensional conductive heat flux in fin
$q_{\text{g,conv}}$	one-dimensional convective heat flux from gas
$q_{\text{g,rad}}$	one-dimensional radiative heat flux from gas
$q_{\text{p,cond}}$	one-dimensional conductive heat flux in pipe
$q_{\text{w,conv}}$	one-dimensional convective heat flux from water
$q_{\text{radiation}}$	one-dimensional radiative heat flux
$\boldsymbol{R}$	randomized value in range 0..1
Re_D	Reynolds number
s	distance in between elements

t	time spent on calculation process
t_{f}	fouling thickness
t_{fin}	fin thickness
t_p	pipe thickness
T	temperature
T_i	temperature at index i
$T_{p,x}$	pipe temperature at x-coordinate
$T_{\mathrm{f,surface}}$	fouling layer temperature at layer surface
T_{g}	gas temperature
T_{surface}	surface temperature
T_w	water temperature
u	velocity
U_p	heat resistivity
$\boldsymbol{v}$	particle velocity vector
V	averaged velocity
W	economizer width
H	economizer height
x	coordinate value in x-axis
$\boldsymbol{x}$	particle design variable vector
x_{fin}	coordinate value in x-axis in fin
x_p	coordinate value in x-axis in pipe
y	coordinate value in y-axis
z	coordinate value in z-axis

GREEK SYMBOLS

v_{h2o}	water vapor volume fraction
v_{co2}	carbon dioxide volume fraction
α	thermal diffusivity
Δp	pressure loss
Δp_{acc}	pressure loss from acceleration
Δp_{fric}	pressure loss from friction
$\Delta p_{\mathrm{increase}}$	pressure loss percentage change
$\Delta p_{\mathrm{minor}}$	pressure loss from minor losses
$\Delta p_{\mathrm{ref,fric}}$	reference pressure loss from friction
ΔT	temperature difference
ϵ	emissivity
ϵ_{total}	total emissivity
ϵ_{H2O}	water vapor Hottel emissivity
ϵ_{CO2}	carbon dioxide Hottel emissivity
η	dynamic viscosity
ϕ	heat transfer rate
ϕ_i	heat transfer rate by substance i
ϕ'	heat transfer rate per meter length
ϕ'_{total}	total heat transfer rate per meter length
ρ	density
σ	Stefan-Boltzmann constant
τ_s	shear stress
$\theta_{p,x}$	temperature difference in between x coordinate and refence coordinate
υ	kinematic viscosity

1. INTRODUCTION

The topic of the present master thesis is to generate an optimization model for Valmet Technologies Oy featuring mass optimization of an economizer geometry in a recovery boiler. Economizers are massive heat exchangers weighting up to hundreds of thousands of kilograms and can exceed tens of meters in length, width and depth. By optimizing the mass of an economizer while retaining the heat transfer rate, large savings can be made in material, manufacturing and erection costs. The thesis consists of building a new 1-dimensional heat transfer model and using a modification of an existing optimization algorithm for finding the optimal solution for the case. The model will be derived from the fundamentals of heat transfer in Chapter 4.

In previous studies, optimization development has already been carried out in similar applications such as fins [1],[2]. As a general remark, many of the heat transfer devices in use have not been optimized and are probably working at low efficiency rates. Thus, optimization is necessary and recently has become a convenient tool.

For the present study, optimization of a large object such as an economizer is a non-trivial task. Aside from the size, problems lie in the sheer number of design variables included. For someone to be able to deduct the effect of several simultaneous geometrical changes to properties such as final mass, heat transfer coefficients and flow profiles, is next to an impossible feat. Therefore, a natural solution is to build a calculation model for the case and observe the results.

1.1 Models for calculation

In order to calculate heat transfer for an economizer geometry, there are several existing ways one may attempt to use. From Computational Fluid Dynamics (CFD), commercial programs such as ANSYS Fluent and its Open Source rival OpenFoam offer solvers for the case. Analytical methods, such as Number of Transfer Units (NTU**)** and Logarithmic Mean Temperature Difference (LTMD), have been generated for fast evaluation of heat transfer machinery. However, the mentioned methods are missing some requirements, such as particle radiation in analytical methods and computational time in CFD calculation. Therefore, a new model must be created.

1.1.1 Problems with current models

The key requirements for this study are low computational time and validity of heat transfer rates of optimized geometries. In CFD, the main problems are with the size of an

economizer. Calculation of even a single case may take up to weeks or months and therefore optimization, which requires multiple cases of calculation, is out of question. From analytical methods, LMTD method is limited in not taking radiation into account. This is troublesome, because high temperature gas mixtures containing water vapor and carbon dioxide induce particle radiation, which may be up to 40 % [3] of the overall heat transfer coefficient. To correct this, a similar model to LMTD was made called Log Mean Heat Transfer Rate (LMHTR) [3]. LMHTR takes radiation into account, but was generated for circular ducts without fins and therefore is not applicable for this case. The second mentioned model, NTU method, expects an infinitely long heat exchanger, which is suitable in the case of an economizer, but also expects a constant overall heat transfer coefficient. For changing constant properties and effect of the exponent of four in radiation, the assumption may be too rigorous and sensitivity analysis should be carried out before actual usage of NTU.

Due to problems with current methods, a new 1-dimensional heat transfer model featuring radiation, changing constant properties and fast computational speed is generated in the present study. Considerable savings in building costs and material requirements as well as general guidelines were found out while carrying out the calculations.

1.2 Thesis Breakdown

In the present master's thesis, Chapter 2 provides general information on an economizer and geometry in the present study. Afterwards, Chapter 3 explains the basics of heat transfer and parameters related to building the heat transfer model. Chapters 4 and Chapter 5 feature building of the heat transfer model and optimization algorithm. Chapter 6 explains details about building the optimization program and calculation process charts. Finally, Chapter 7 presents results obtained from the generated model and they are later discussed in Chapter 8 with possible future research plans.

2. ECONOMIZERS IN RECOVERY BOILERS

Economizers are generally long and massive heat exchangers consisting of cast tubes and a flow channel around the tubes. Heat is transferred in between the fluid inside the tubes and the fluid in the channel. The aim for an economizer is to increase efficiency of a boiler by using flue gas from the boiler to preheat water entering the boiler.

2.1 General overview

Economizers are constructed from materials with relatively good heat conductivity and tolerance for high temperatures, such as steel and other metals. High temperature flue gas led from the boiler into the economizer. Simultaneously low temperature high pressure water is led from feedwater tank into the economizer, as shown in Figure 1. After economizers the flue gas is processed in electrostatic precipitator and is then released into atmosphere.

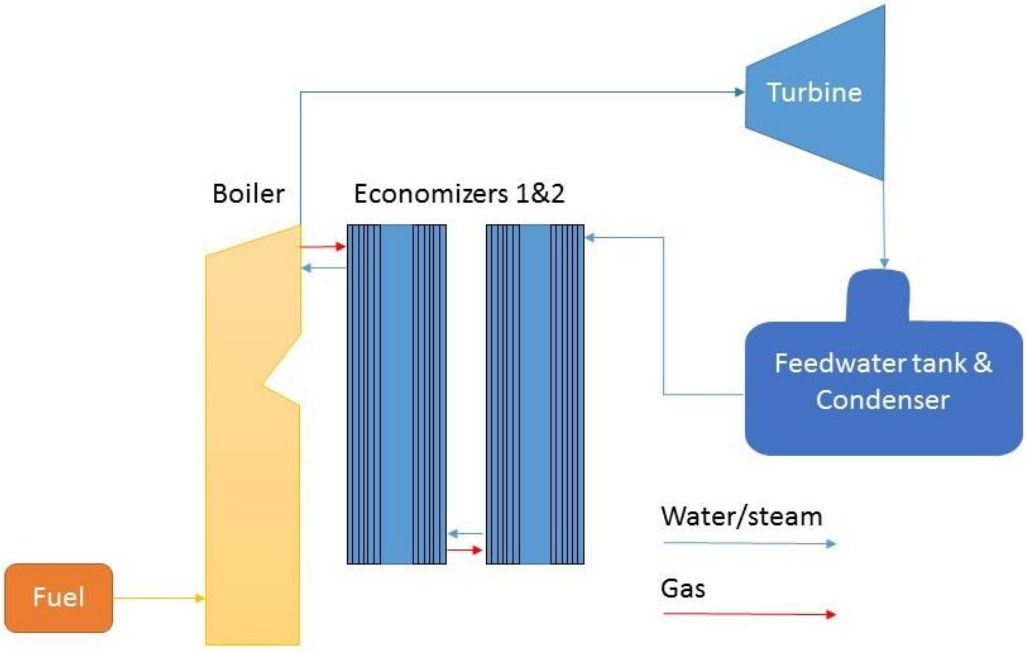

Figure 1. *Recovery Boiler process chart*

Inside an economizer, heat is transferred from gas to water by a combination of convective, conductive and radiative heat transfer. The flows are separated by tube walls, which usually have fins attached in order to enhance heat transfer. The flue gas is a product of burning black liquor as fuel, and is a gas component mixture consisting mainly of carbon

dioxide (CO_2), water (H_2O), oxygen (H_2O) and nitrogen (N_2). Water entering the economizer has been pressurized in the feedwater tank for tolerating high temperatures. As for a more realistic picture, a typical layout for an economizer would be as shown in Figure 2.

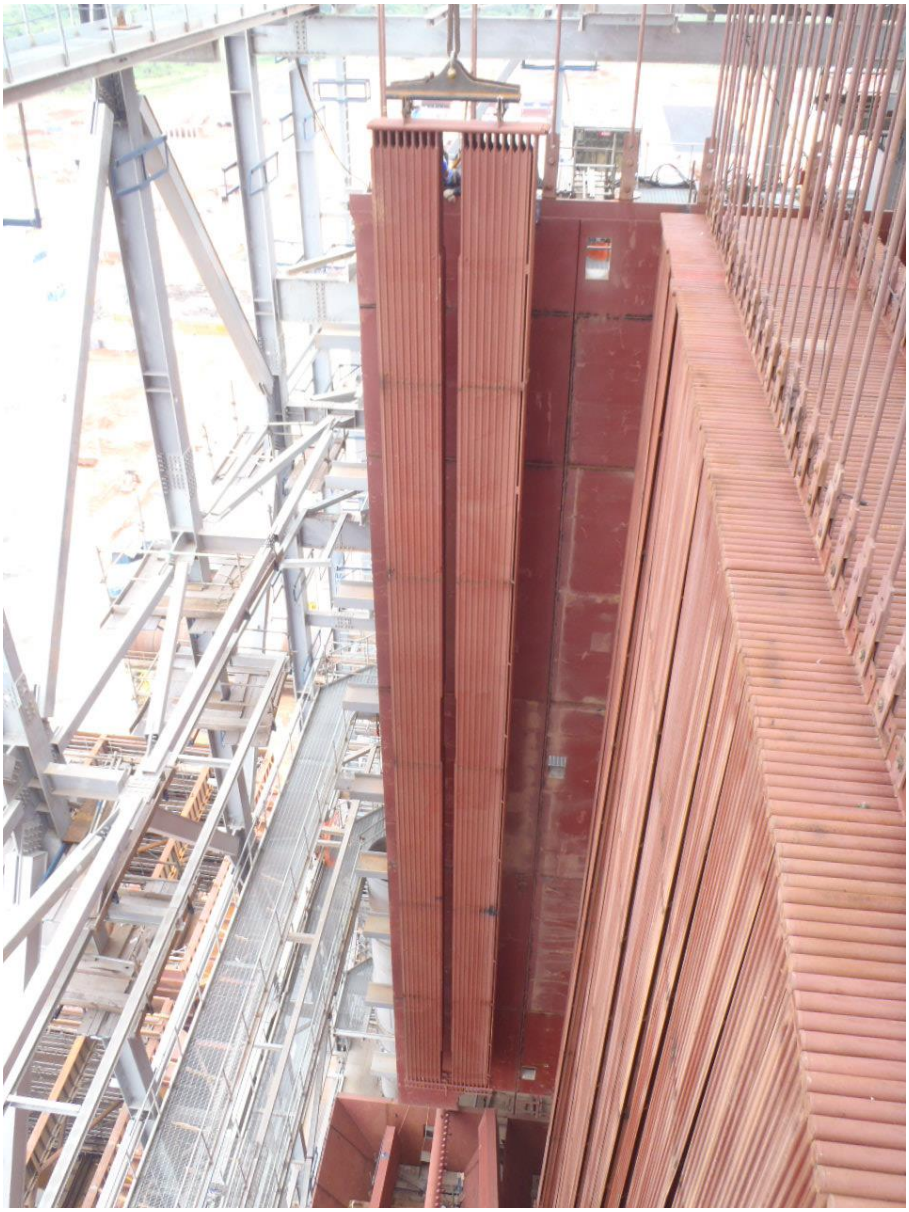

Figure 2. *Economizer installation, Valmet Technologies Oy*

In Figure 2 pipe packets have a sootblowing cavity in between for cleaning the body material from salt deposits. The fouling of the surface material reduces heat transfer by acting as a thermal resistance and thus, lowering the total efficiency of the economizer. In historical notes, fouling was a serious problem in first recovery boilers built [4]. Sootblowing cavities are used for periodical cleanup of the economizers. Periodical cleanup decreases the interval in between full cleanup allowing longer usage times for the economizer and therefore to the recovery boiler.

2.1.1 Flow configurations

There are a number of flow configurations available for a two-fluid flow heat exchanger of which the most common are parallel-flow, counter-flow and cross-flow designs. The configurations have advantages over one another. In the first option of parallel-flow design, the fluids flow parallel in the same direction resulting in great temperature differences at the inlets while giving similar end temperatures for both. This is shown in Figure 3, where T stands for temperature, subscript h denotes high temperature fluid and subscript c is for low temperature fluid.

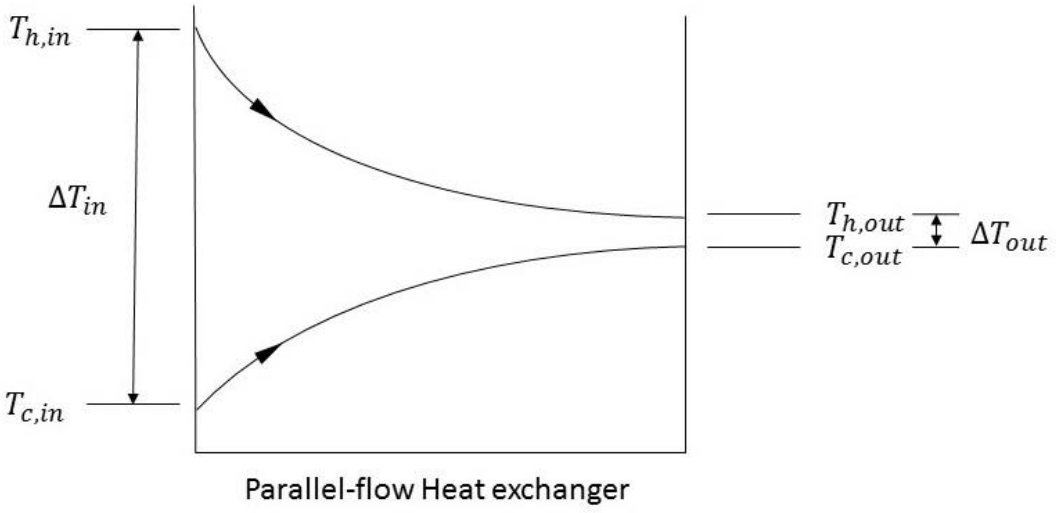

Figure 3. *Parallel-flow heat exchanger*

The second option, counter-flow design, offers higher heat transfer rate and more uniform heat flux in comparison to parallel-flow configuration. The fluids flow in opposite direction in counterflow setup. Temperature differences at both ends of the economizer are low and result in less thermal stresses. The temperature change for a counterflow economizer can be expressed as shown in Figure 4.

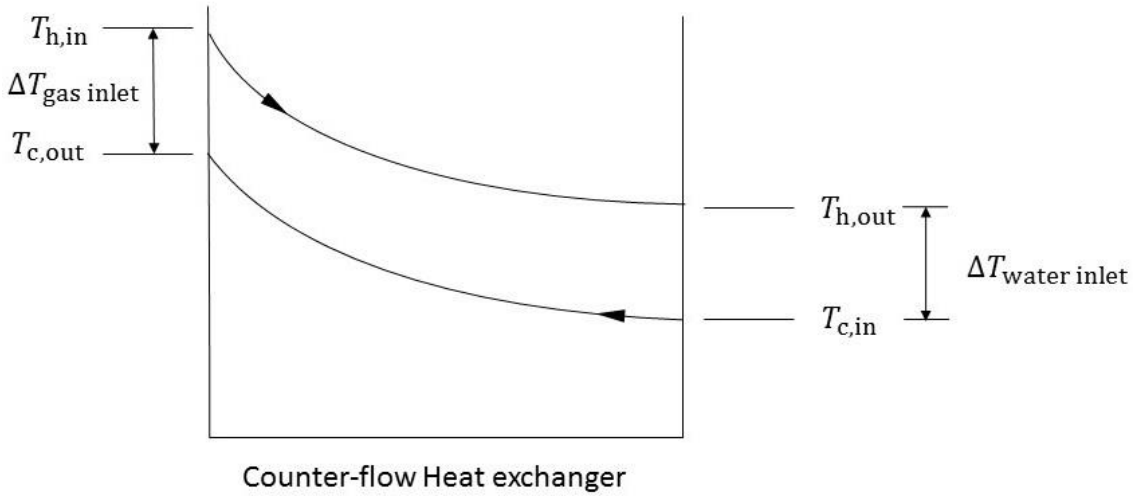

Figure 4. *Counterflow Heat exchanger*

The third configuration option, cross-flow design, can be either parallel- or counterflow based. It has been recorded to be more efficient than normal counterflow, but can be combined with either parallel-flow or cross-flow configuration. In a cross-flow setup counterflow has been recorded to have higher heat transfer than parallel-flow configuration [5]. However, cross-flow design is more troublesome due to horizontal tubes acting as "shelves" or platforms increasing the fouling rate.

2.1.2 Material and geometric requirements

A set of requirements must be met when building an economizer. The initial one is to raise water temperature to a certain level while meeting requirements for maximum pressure drop allowed. The pressure drop is directly proportional to power required for pumping gas thus affecting total power consumption. Temperature change on other hand can be directly translated to heat transfer, which affects total efficiency of the recovery boiler. Both pressure loss and heat transfer rate can be altered by changing the geometry, mass flows and inlet temperatures.

Materials used in construction is required to have good thermal and mechanical resistance as well as good thermal conductivity to enhance heat transfer. Metals such as carbon steel and stainless steel are often used being cheaper in price compared to metals with higher heat conductivity like copper. Carbon steel is often preferred over stainless steel due to lower material costs.

2.1.3 Experimental data

Experimental data can be gathered from previously made economizers but can be hard to obtain from anywhere else than the inlet and the outlet. With water, the measuring will be very accurate, but when measuring temperature of the gas mixture, the results will be

uncertain. This is because of three mains reasons. The first problem arises if the gas temperature is not even at the measurement point, which is very normal as the point of measurement is usually located near a wall. The second one is radiation, which can cause too high numbers in thermometer if not protected. The third reason is due to the fouling of the thermometer itself, which results as higher overall heat resistance in between the fluid and the thermometer.

2.2 Geometry in the present study

Chapter 2.1.1 explained possible flow configurations for an economizer. The model in used in this study is a pipe-fin two-fluid counterflow heat exchanger featuring water heat-up with exhaust fumes.

2.2.1 Configuration

The full economizer shown in Figure 5 A) consists of several pipe-fin elements described in Figure 5 B). Figure 5 C) shows a welded connection in between pipes and fins.

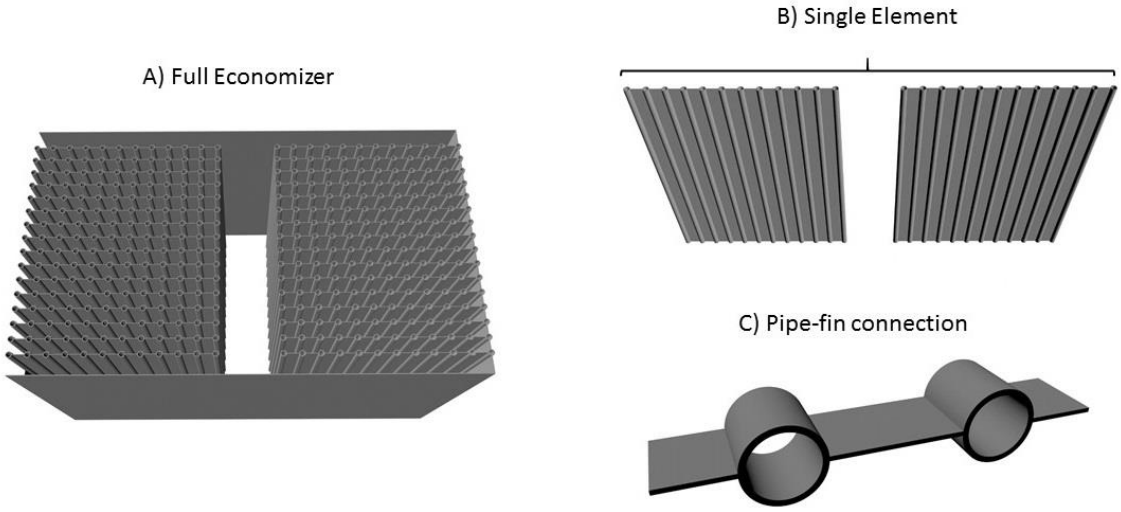

Figure 5. *Full economizer (a), single element (b), pipe-fin connection (c)*

Sootblowing cavity in the economizer can be seen in between the two parts of a single element in Figure 5 B), and in the gap shown in the full economizer configuration of Figure 5 A).

2.2.2 Flow profile and direction

The flow directions and estimate profiles are shown in Figure 6 an the geometry of drawn picture is further clarified with Figure 6.

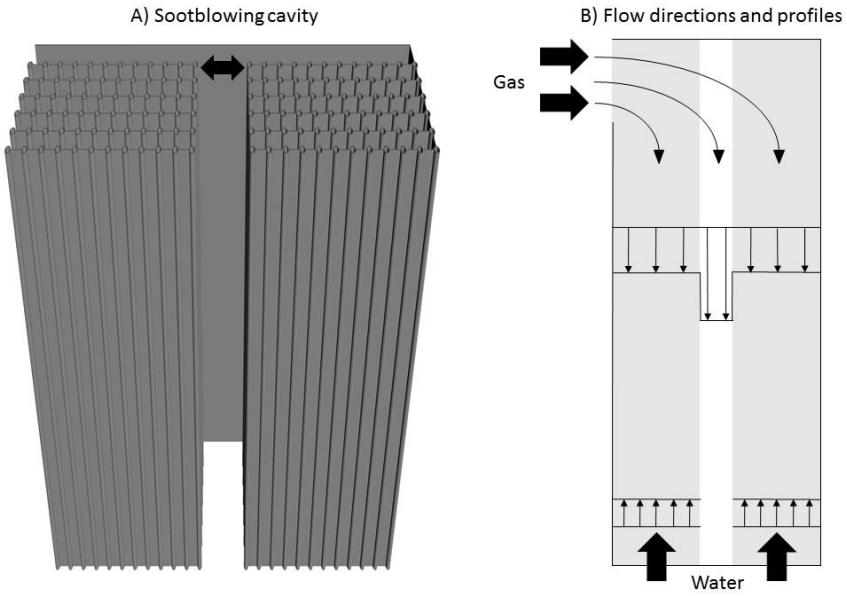

Figure 6. *Sootblowing cavity (a), flow directions and profiles (b)*

Water is expected to have a uniform velocity perpendicular to streamwise direction. As for gas velocity profile, sootblowing cavity is expected to have a faster velocity in comparison to flow within the pipe-fin –region. Relation of the flow speeds in sootblowing cavity and pipe-fin –region are further discussed and evaluated in 4.5.

3. THEORY

This chapter contains the fundamental aspects of calculating heat transfer, parameters related to heat transfer, and evaluation of pressure drop and fluid temperature change.

3.1 Heat transfer

Heat is transferred by three different ways: conduction, convection and radiation. According to J.B. Fourier Mills [5], conductive heat flux $q_{\text{conduction}}$ within a material can be expressed as

$$q_{\text{conduction}} = -k\frac{\mathrm{d}T}{\mathrm{d}x} \tag{1}$$

where k is thermal conductivity of the body material, T temperature of the material and x denotes the position in the direction of heat transfer. The minus sign describes that heat is transferred in the direction of lower temperature.

Convection is heat transfer between a fluid and a solid. In conjunction with thermal conductivity k, the convection coefficient h is used and convective heat flux $q_{\text{convection}}$ can be defined as [5]

$$q_{\text{convection}} = h\Delta T \tag{2}$$

where ΔT is the temperature difference between a solid surface and a fluid.

Radiation exchange between an isothermal gray gas mixture and a grey surface can be expressed as [5]

$$q_{\text{radiation}} = \varepsilon\sigma(T_{\text{g}}^4 - T_{\text{surface}}^4) \tag{3}$$

where $q_{\text{radiation}}$ is the radiative heat flux, σ is Stefan-Boltzmann constant and ε emissivity of the gas. For simplicity, an approximation is made that surface absorbs all radiation emitted by gas. [5]

3.2 Evaluation of flow and heat transfer parameters

The most important parameters in heat transfer and flow evaluation are Reynolds number Re and Nusselt number Nu. Reynolds number can single-handedly give estimation on whether a flow can be estimated as turbulent or laminar. Reynolds number can be defined as

$$\mathrm{Re_D} = \frac{U d_\mathrm{h}}{\nu} \tag{4}$$

where U is velocity of the medium, d_h is hydraulic diameter of the geometry and ν is the medium kinematic viscosity. Forced flow in a pipe can be considered as turbulent if Reynolds number $\mathrm{Re} > 2300$ [5]. With a flow between two flat plates, a safe estimation would be when $\mathrm{Re} > 5000$. In equation (4) hydraulic diameter can be expressed as follows

$$d_\mathrm{h} = \frac{4A}{P} \tag{5}$$

where A is cross-sectional area perpendicular to fluid flow direction and P is the perimeter. In the present study we will find that Reynolds number stays in the turbulent area. For a turbulent flow, there are a number of ways to calculate Nusselt number and Gnielinski correlation has proven to be a good estimation. It can be described as

$$\mathrm{Nu_D} = \frac{\left(\frac{\mathrm{f}}{8}\right)(\mathrm{Re_D} - 1000)\mathrm{Pr}}{1 + 12.7\left(\frac{\mathrm{f}}{8}\right)^{\frac{1}{2}}\left(\mathrm{Pr}^{\frac{2}{3}} - 1\right)} \tag{6}$$

in which Pr denotes the Prandtl number and f means the friction factor of material. The results of Gnielinski correlation are valid when $3000 > Re > 10^6$ and has an accuracy of 20% to experimental results within this region [5]. For evaluation of smooth material, the friction factor can be estimated from correlation made by Petukhov [5] as

$$\mathrm{f} = \left(0.790 * \ln\left(Re_{\mathrm{D_h}}\right) - 1.64\right)^{-2} \tag{7}$$

which is valid when $10^4 < \mathrm{Re_{D_h}} < 10^6$. Both Gnielinski correlation and correlation made by Petukhov were intended for circular ducts, but can be implemented for flow between parallel plates with good accuracy. Alternatively, if absolute roughness is known for a material, the friction factor can be estimated from Moody Chart shown in Figure 7. [5]

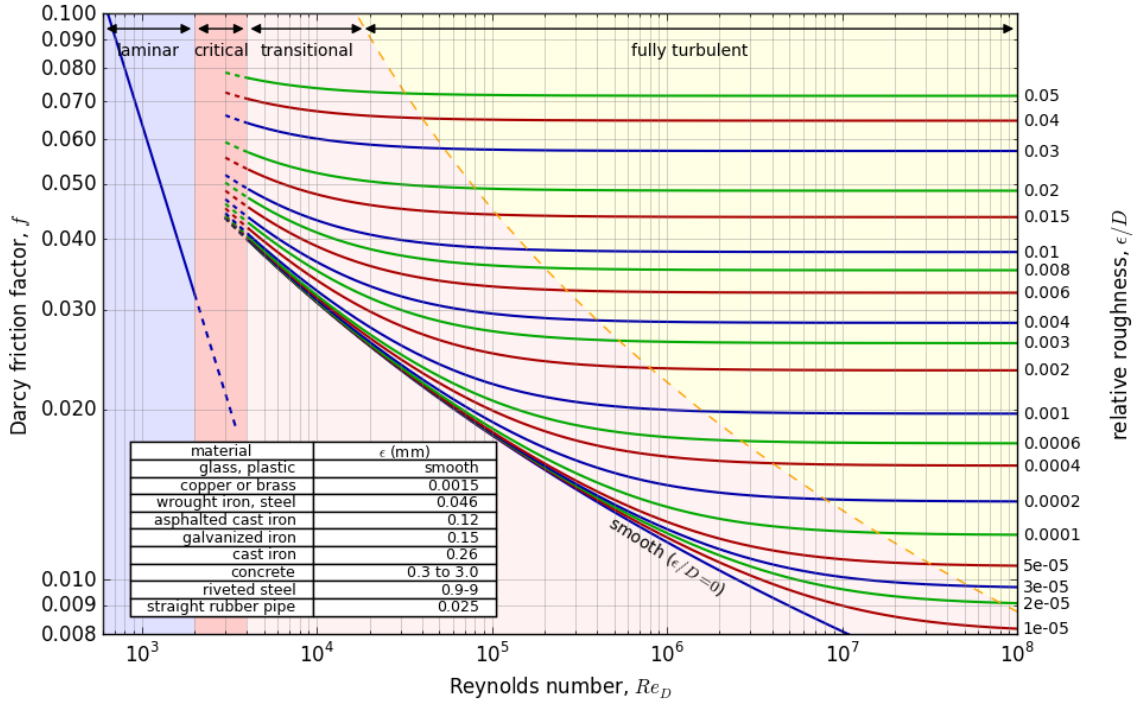

Figure 7. *Moody Diagram*

Alternatively, friction factor can be gotten from Colebrook-White Equation [6], which has the form of

$$\frac{1}{\sqrt{\mathrm{f}}} = -2\ \log\left(\frac{\epsilon_{\mathrm{r}}}{3{,}7d_h} + \frac{2{,}51}{\mathrm{Re}_D\sqrt{\mathrm{f}}}\right) \tag{8}$$

where ϵ_{r} represents surface roughness.

Prandtl number can be calculated by dividing fluid kinematic viscosity ν with its thermal diffusivity α as

$$\mathrm{Pr} = \frac{\alpha}{\nu} \tag{9}$$

For wide range of gases, Pr can be assumed to be of value 0.7 even at higher temperatures. For water, the Prandtl number value varies at high pressures with temperature changes and must be evaluated more carefully.

From Nusselt number we can define heat transfer coefficient as

$$h = \frac{Nu_{\mathrm{d}}k}{d_{\mathrm{h}}} \tag{10}$$

which we can then apply to calculate heat flux with equation (2).

The emissivity ε for calculating radiation can be estimated from Hottel charts [5] as a function of mean path length $\bar{l}$ and temperature T. Mean free path length can be calculated as

$$\bar{l} = \frac{k_b T}{\sqrt{2}\pi p_{\mathrm{g}} d_{\mathrm{m}}^2} \tag{11}$$

Where k_b is Boltzmann constant, p_{g} is pressure and d_{m} is molecular diameter.

Hottel charts are presented for water and carbon dioxide, which take part in particle radiation. Figure 8 a) shows carbon dioxide emissivity and Figure 8 b) shows water vapor emissivity in correspondence to temperature and path length of the gas.

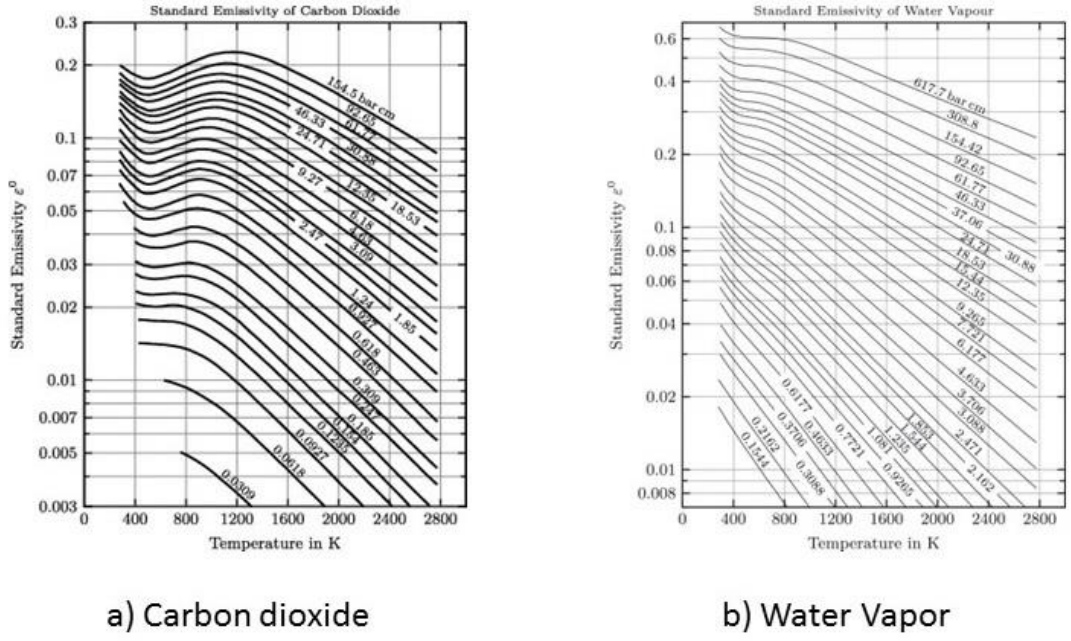

a) Carbon dioxide b) Water Vapor

Figure 8. *Spectral emissivity for a) carbon dioxide, b) water vapor [5]*

With emissivity for water vapor and carbon dioxide from charts, we can then calculate total emissivity for the gas mixture by volume fractions as

$$\varepsilon_{\mathrm{total}} = \varepsilon_{\mathrm{h_2o}} v_{\mathrm{h_2o}} + \varepsilon_{\mathrm{co_2}} v_{\mathrm{co_2}} \tag{12}$$

where v denotes volume fraction of substance in gas mixture.

3.3 Pressure drop evaluation

Evaluation of pressure drop is important as it affects power needed in order to pump the gas into the economizer. Pressure drop is a sum of pressure drop by friction Δp_{fric}, pressure loss from minor losses Δp_{minor} and pressure loss from acceleration Δp_{acc} as shown in Equation (13).

$$\Delta p = \Delta p_{\text{fric}} + \Delta p_{\text{minor}} + \Delta p_{\text{acc}} \tag{13}$$

Minor losses in the economizer are hard to calculate due to complex inflow configuration and pressure loss by acceleration can be neglected being minor in comparison to pressure loss by friction. Pressure loss through friction can be calculated evaluated with Equation (14)

$$\Delta p_{\text{fric}} = 4\text{f}\frac{1}{2}\rho V^2 \frac{L}{d_{\text{h}}} \tag{14}$$

where ρ represents density of the fluid [7]. Equation (14) can be deducted from the equation for shear stress

$$\tau_{\text{s}} = \eta \frac{\partial u}{\partial y} \tag{15}$$

where η is dynamic viscosity and τ_{s} shear stress. The relation between friction factor and shear stress can be defined as stated below in equation (16).

$$\text{f} = \frac{\tau_{\text{s}}}{\frac{1}{2}\rho V^2} \tag{16}$$

Equation (14) has been originally expressed for flow inside a circular duct, but can be implemented for a flow between two parallel flat plates if the flow is in turbulent region. The current model is close to a parallel-plate configuration, so Equation (14) is believed to show reliable results. However, because roughness for salt deposits cannot be known, the results must be evaluated for a clean economizer with the roughness of body material. This way new pressure loss can be estimated as percentage $\Delta p_{\text{increase}}$ increase from a known model pressure loss by friction $\Delta p_{\text{ref,fric}}$ with Equation (17)

$$\Delta p_{\text{increase}} = \frac{\Delta p_{\text{fric}} - \Delta p_{\text{ref,fric}}}{\Delta p_{\text{ref,fric}}} \tag{17}$$

By assuming friction factor f and density ρ as constant for both Δp_{fric} and $\Delta p_{ref,fric}$, percentage increase in pressure losses by friction are only a factor of squared velocity V^2,

length L and hydraulic diameter d_{h}. Thereby pressure loss by friction for a new economizer can be calculated as show in Equation (18).

$$\Delta p_{\mathrm{fric}} = \Delta p_{\mathrm{increase}} \Delta p_{\mathrm{ref,fric}} + \Delta p_{\mathrm{ref,fric}} \tag{18}$$

4. CALCULATION MODEL

In this chapter, a streamwise one-dimensional model is created for calculation of total heat transfer. Assumptions regarding approximations will be explained.

4.1 Governing equations

In the one-dimensional model, two basic laws govern the whole calculation region; law of conservation of mass and law of conservation of energy. Law of conservation of mass states that mass cannot be created or cannot disappear within the flow. In one-dimensional it can be described as

$$\frac{\partial(\rho u)}{\partial x} = 0 \tag{19}$$

where ρ is density of the fluid, u velocity and x denotes position in streamwise direction.

Law of conservation of energy states that total energy of an isolated system stays constant. In the heat transfer system, we form this in the way that all heat transfer occurs between the two fluid mediums, meaning no heat is stored and system is considered as stationary. The energy transferred to and from fluid can be written as

$$\phi = \dot{m} c_{\mathrm{p}} \Delta T \tag{20}$$

where ϕ is heat transfer rate, $\dot{m}$ mass flow and c_p specific heat capacity. Stationary condition can be stated as

$$\sum \phi_{\mathrm{i}} = 0 \tag{21}$$

where subscript i denotes a fluid medium in the system.

4.2 Fouling approximation

In usage of the economizer, ash particles in the gas causes fouling on the surfaces of material used in construction. Thickness of the fouling layer varies and therefore would be easier to approximate as a layer of constant thickness and constant conduction coefficient throughout the economizer. The conduction coefficient can be measured in practice with means of temperature measurement in closed conditions. The thickness of the fouling layer will be evaluated through comparison of the calculations with experimental data. It is convenient to assume one dimensional heat flow through fouling layer for simplicity of calculation.

4.3 Heat flow

In generating the one-dimensional model, streamwise heat transfer rate per meter is solved and uniform temperature distribution in fluids perpendicular to the flow direction is assumed. The heat flow from gas to water through fouling layer and material surface can be estimated, if they are treated separately as shown in figure Figure 9.

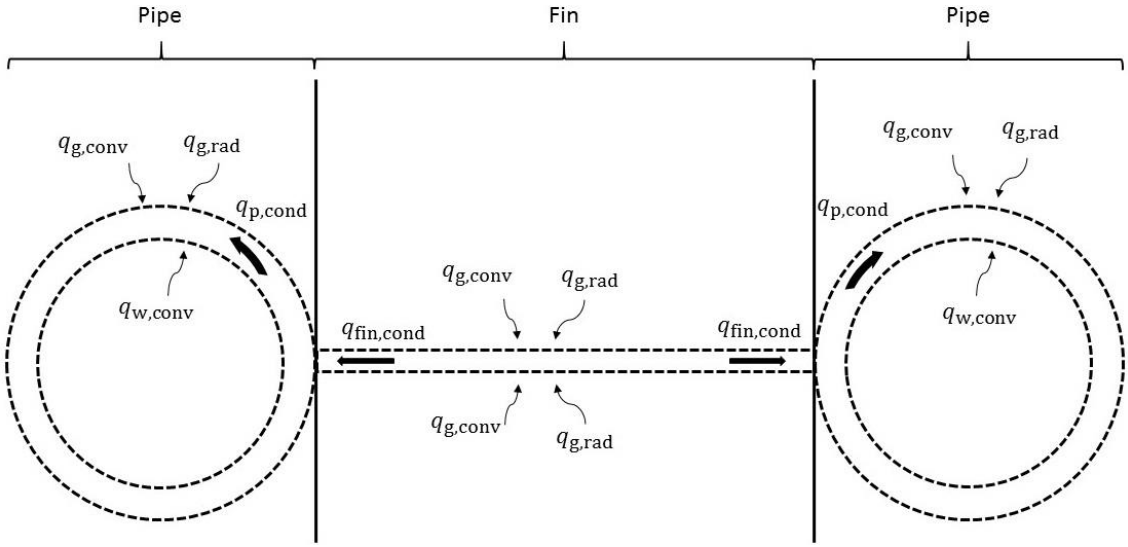

Figure 9. *Pipe-fin division to pipe and fin*

In Figure 9 $q_{g,conv}$ stands for convection from gas, $q_{g,rad}$ radiation from gas, $q_{\mathrm{fin,cond}}$ conduction in fin, $q_{\mathrm{p,cond}}$ conduction in pipe and $q_{w,conv}$ convection from water. The connection point of pipe and fin is considered as boundary condition for temperature in calculation. In the pipe-section heat conduction $q_{\mathrm{p,cond}}$ in economizer material equals to heat flow to water $q_{\mathrm{w,conv}}$ and conduction from fouling layer $q_{\mathrm{f,cond}}$. In the fin-section, conduction $q_{\mathrm{fin,cond}}$ in material equals to conduction from fouling layer. Heat balance for pipe-section material can be estimated by using a control volume as shown in Figure 10 (a) and for fin section as shown in Figure 10 (b).

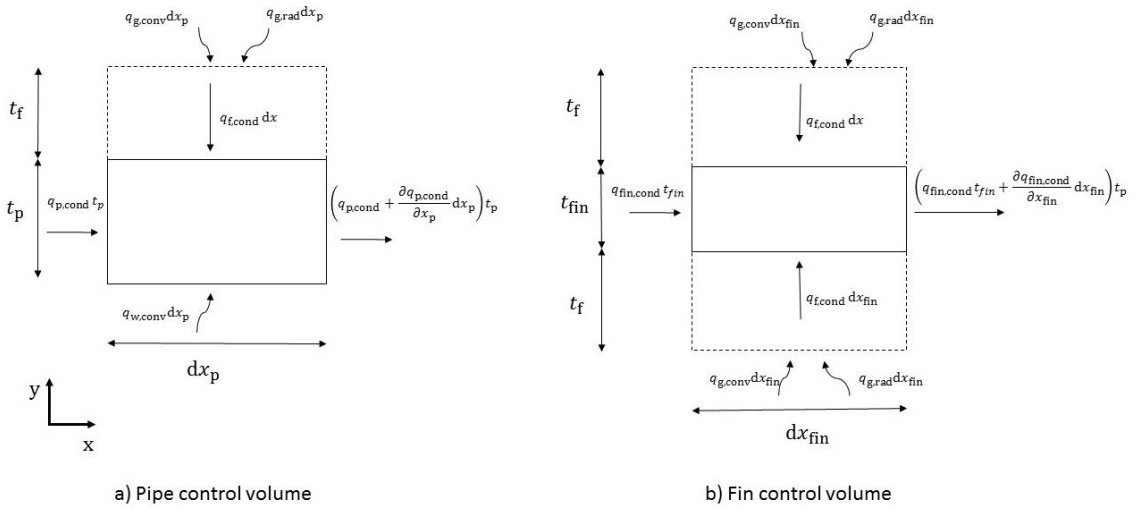

Figure 10. *Control volume for pipe material (a), control volume for fin (b)*

In Figure 10 t_f stands for fouling layer thickness, t_p pipe thickness and t_fin fin thickness. One dimensional conduction is assumed in fouling layer y-direction and in economizer material x-direction. Heat balance per meter length for pipe material can be written as

$$\frac{\partial q_{\mathrm{p,cond}}}{\partial x_\mathrm{p}}\mathrm{t_p d}x_\mathrm{p} = \left(q_{\mathrm{f,cond}} - q_{\mathrm{w,conv}}\right)\mathrm{d}x_\mathrm{p} \tag{22}$$

Further, the conduction from fouling layer is equivalent to heat transferred from gas by radiation and convection as stated below

$$q_{\mathrm{f,cond}} = q_{\mathrm{g,conv}} + q_{\mathrm{g,rad}} \tag{23}$$

By merging equations (2) and (3) we can rewrite equation (23) as

$$q_{\mathrm{f,cond}} = \frac{1}{\frac{1}{h_\mathrm{g} + \sigma\varepsilon\left({T_\mathrm{g}}^2 + {T_{\mathrm{f,surface}}}^2\right)\left(T_\mathrm{g} + T_{\mathrm{f,surface}}\right)} + \frac{k_\mathrm{f}}{t_\mathrm{f}}}\left(T_\mathrm{g} - T_{\mathrm{p,x}}\right) \tag{24}$$

where k_f refers to thermal conductivity of fouling layer and $T_{\mathrm{p,x}}$ is the temperature of pipe at coordinate x. The value of fouling temperature at surface can be iterated from equations (23) and (24). By marking U_p as

$$U_\mathrm{p} = \frac{1}{\frac{1}{h_\mathrm{g} + \sigma\varepsilon\left({T_\mathrm{g}}^2 + {T_{\mathrm{f,surface}}}^2\right)\left(T_\mathrm{g} + T_{\mathrm{f,surface}}\right)} + \frac{k_\mathrm{f}}{t_\mathrm{f}}} \tag{25}$$

we can write equation (22) as

$$-t_{\mathrm{p}}\frac{\partial q_{\mathrm{p,cond}}}{\partial x_{\mathrm{p}}}=U_{\mathrm{p}}\left(T_{\mathrm{g}}-T_{\mathrm{p,x}}\right)+h_{\mathrm{w}}\left(T_{\mathrm{w}}-T_{\mathrm{p,x}}\right) \tag{26}$$

Where h_{w} is convection coefficient of water and T_{w} is water temperature and it translates to

$$\frac{\partial^2 T_{\mathrm{p}}}{\partial^2 x_{\mathrm{p}}}=\frac{h_{\mathrm{p,eff}}}{t_{\mathrm{p}}k}\left(T_x-\frac{UT_{\mathrm{g}}+h_{\mathrm{w}}T_{\mathrm{w}}}{h_{\mathrm{p,eff}}}\right) \tag{27}$$

where $h_{\mathrm{p,eff}}=U_{\mathrm{p}}+h_{\mathrm{w}}$. By selecting $\theta_{\mathrm{p,x}}$ as

$$\theta_{\mathrm{p,x}}=T_{\mathrm{p,x}}-\frac{UT_{\mathrm{g}}+h_{\mathrm{w}}T_{\mathrm{w}}}{h_{\mathrm{p,eff}}} \tag{28}$$

and ${m_{\mathrm{p}}}^2=\frac{h_{\mathrm{p,eff}}}{t_{\mathrm{p}}k}$ we get the temperature profile of the pipe material, which is also the standard fin equation and can be written as

$$\theta_{\mathrm{p,x}}=\frac{\cosh\left(m_{\mathrm{p}}\left(\frac{\frac{l_{\mathrm{p}}}{2}-x_{\mathrm{p}}}{2}\right)\right)}{\cosh\left(m_{\mathrm{p}}\frac{l_{\mathrm{p}}}{4}\right)}\theta_{\mathrm{p,0}} \tag{29}$$

where l_{p} is the averaged perimeter of pipe. For the fin-section control volume in Figure 10 (b), the heat balance can be written as

$$\frac{\partial q_{\mathrm{fin,cond}}}{\partial x_{\mathrm{fin}}}\mathrm{t}_{\mathrm{fin}}\mathrm{d}x_{\mathrm{fin}}=2q_{\mathrm{f,cond}}\mathrm{d}x_{\mathrm{fin}} \tag{30}$$

Similarly to achieving (29), we get the temperature distribution for the fin section, which can be written as

$$\theta_{\mathrm{fin,x}}=\frac{\cosh\left(m_{\mathrm{fin}}\left(\frac{l_{\mathrm{fin}}}{2}-x_{\mathrm{fin}}\right)\right)}{\cosh\left(m_{\mathrm{fin}}\frac{l_{\mathrm{fin}}}{2}\right)}\theta_{\mathrm{fin,0}} \tag{31}$$

Where l_{fin} is the fin length, $m_{\mathrm{fin}}=\frac{2h_{\mathrm{fin,eff}}}{t_{\mathrm{fin}}k}$, $\theta_{\mathrm{fin}}=T_{\mathrm{fin,x}}-T_{\mathrm{g}}$ and $h_{\mathrm{fin,eff}}=U_{\mathrm{fin}}=U_{\mathrm{p}}$.

By marking boundary condition for the intersection point as $\theta_{\mathrm{fin,0}}=\theta_{\mathrm{p,0}}$, the temperature profile for both sections can be solved. Intersection temperature can be iterated by marking heat absorbed by water the same as heat given by gas $\phi_w'=\phi_g'$. Heat absorbed by water ϕ_w' is written as

$$\phi'_w = \int_0^{\mathrm{l_p}} q_{\mathrm{w,conv}} \mathrm{d}x_p \tag{32}$$

Heat given out by gas ϕ'_g can be written as

$$\phi'_g = \int_{-l_\mathrm{p}}^{l_\mathrm{p}} q_{\mathrm{f,cond}} \mathrm{d}x_\mathrm{p} + \int_0^{\mathrm{l_{fin}}} q_{\mathrm{f,cond}} \mathrm{d}x_\mathrm{fin} \tag{33}$$

Because of the 4th order exponent from radiation, there is not direct way to solve either integration. Instead, the integrals will be divided into sums of linearized temperature distributions as shown in Equation (34)

$$\phi'_\mathrm{total} = \sum_{i=0}^{k} q_\mathrm{i} \mathrm{d}x_\mathrm{i} \tag{34}$$

Once the heat absorbed by water equals to heat given by gas $\phi'_{\mathrm{g,total}} = \phi'_{\mathrm{w,total}}$, the temperature profile is correct and heat transferred by economizer length meter has been found.

4.4 Streamwise fluid temperature change

After temperature profile has been found, knowing that total heat transferred by economizer ϕ equals to heat transfer by meter of economizer ϕ' integrated by economizer length ∂z

$$\phi = \int \phi' \, \partial z \tag{35}$$

We can calculate temperature change by equation (20) as

$$c_\mathrm{p} \dot{m} \, \partial T = \phi' \, \partial z \tag{36}$$

For a short distance we can approximate a linear relation $\frac{\partial T}{\partial z} \approx \frac{\Delta T}{\Delta z}$ and thus get the fluid temperature change as shown in equation (37), which is the one dimensional model for temperature change.

$$T_{\mathrm{i+1}} = \frac{\phi'}{c_\mathrm{p} \dot{m}} \Delta z + T_\mathrm{i} \tag{37}$$

For each step in economizer length, both water and gas temperatures must be known. In the counter-flow setup we only know inlet temperatures, in which case we have to iterate through the economizer in order to find the correct end temperature for the guessed value.

4.5 Sootblowing cavity effect approximation

Calculation for sootblowing cavity effects on heat transfer are taken into account by calculating the pressure losses in both pipefin -region and sootblowing cavity and marking them as equal to each other. From equation (14) we can get

$$\frac{4\mathrm{f}_1 \frac{1}{2}\rho_1 V_1^2 L}{d_{\mathrm{h}_1}} = \frac{4\mathrm{f}_2 \frac{1}{2}\rho_2 V_2^2 L}{d_{\mathrm{h}_2}} \tag{38}$$

By approximating f and ρ constant and using law of conservation of mass, we can derive a relation to mass flows within pipefin and sootblowing cavity as

$$\dot{m}_{\mathrm{pipefin}} = \frac{A_{\mathrm{pipefin,gas}}}{A_{\mathrm{cavity}}} \sqrt{\frac{d_{\mathrm{h}_{\mathrm{pipefin}}}}{d_{\mathrm{h}_{\mathrm{cavity}}}}}\, \dot{m}_{\mathrm{cavity}} \tag{39}$$

of which we can achieve the total values by knowing that the total mass flow is the sum of these two mass flows and can be expressed as $\dot{m}_{\mathrm{total}} = \dot{m}_{\mathrm{pipefin}} + \dot{m}_{\mathrm{cavity}}$. From here the values for velocities in both cavity and pipe-fin –region can be estimated. Because of changing flow properties, the values must be calculated for each step in streamwise calculation independently.

The interaction of mass flow in sootblowing cavity with the mass flow in the pipe-fin-region is hard to estimate. We can define two borderlines, of which the first one is that temperatures even out during every step and in the second one the flow in the sootblowing cavity does not interact with the flow in pipe-fin –region.

For solving the problem, the latter case was chosen. The effect of cavity can be expressed as limiting factor to heat transfer and thus may be combined with fouling thickness, which was already an approximated value.

4.6 Gas entrance effect

Gas enters the economizer as shown in Chapter 2, Figure 6. Calculating the gas entrance effect with CFD might be possible, but the results will be questionable because there is no validation for the calculations. For analytical solutions, the problem is nigh impossible to estimate due to same reason. It is assumed that the gas entrance affects minor losses and heat transfer in that region. While the effect of gas entrance to overall heat transfer rate can be included in previously determined fouling thickness by comparing calculation results to experimental results, the effect on minor losses is hard to estimate. This is because of the complex inflow geometry and gas separation on tube walls.

4.7 Simplifying the created 1-dimensional model

Solving the 1-dimensional heat transfer model requires iterations over fouling surface temperature, intersection point and end temperatures, which are all overlapping. To reduce calculation time, it is possible to make approximations, which will be afterwards validated with the original model. The first simplification would be to assume pipe surface temperature uniformly as water temperature. The second simplification would be to neglect calculation of radiation and combine it with the first simplification.

4.7.1 Uniform temperature approximation in pipe

The biggest time consumer in the calculation is iterating over the intersection point in between pipe and fin. By assuming temperature of the pipe body material to be uniform and the same value as water temperature in each section, we can directly assume the intersection to be of this value as well. Assumption derives from expectation, that convection coefficient of water h_{w} is dominative in comparison to overall heat resistivity in between material surface and gas.

With the second simplification, analytical solution can be derived. First we need to assume pipe temperature as water temperature to neglect iteration of intersection temperature. Secondly we neglect radiation, which allows integration of heat flux perpendicular to fluid flow direction in contrast to (33). We can then calculate the heat flow as stated in equation (40)

$$\phi' = \frac{l_{\mathrm{p}} + \frac{4\tanh\left(\frac{\mathrm{m}_{\mathrm{fin}} l_{\mathrm{fin}}}{2}\right)}{\mathrm{m}_{\mathrm{fin}}}}{\frac{t_{\mathrm{f}}}{k_{\mathrm{f}}} + \frac{1}{h_{\mathrm{g}}}} \left(T_g - T_w\right) \tag{40}$$

where $m_{\mathrm{fin}} = \sqrt{\frac{2}{\left(\frac{t_{\mathrm{f}}}{k_{\mathrm{f}}} + \frac{1}{h_{\mathrm{g}}}\right) t_{\mathrm{fin}} k_{\mathrm{fin}}}}$ is heat transfer per economizer meter for a single pipe-fin connection. The analytical solution could possibly speed up the optimization tremendously and reduce a single economizer heat calculation to less than a second. Comparison of simplified solution results with initial model will be presented in Chapter 7.

5. PARTICLE SWARM OPTIMIZATION

Particle Swarm Optimization (PSO) was chosen as the method for optimization. This chapter explains basics of PSO, optimization aim, design variables and reasons for choosing PSO.

5.1 Optimization aim and design variables

The aim of this optimization is to obtain minimum mass $M = M_{\mathrm{min}}$ while retaining heat transfer rate ϕ. The design variables for the case are pipe diameter d, pipe thickness t_{p}, fin length l, fin thickness t_{fin}, spacing in between elements s, economizer total length L, total width W and total height H. The target function can be written as

$$M = f(d, t_{\mathrm{p}}, l, t_{\mathrm{fin}}, s, L, W, H) \tag{41}$$

Heat transfer rate ϕ acts as an inequality constraint and must exceed chosen heat transfer rate amount $\phi \geq \phi_{\mathrm{min}}$. Like mass M, heat transfer rate is a function of design variables. Inequality constraint ϕ_{min} can be written as

$$\phi_{\mathrm{min}} \leq g(d, t_{\mathrm{p}}, l, t_{\mathrm{f}}, s, L, W, H) \tag{42}$$

5.2 Choosing PSO

Several optimization methods can be used for optimization. Three major categories exist, which are gradient-based methods, gradient-free methods and population-based methods [8].

Population-based methods function well in applications that have multiple design variables such as the present study. Furthermore, they are easy to parallelize, because each particle acts independently during an iteration step. PSO seemed as a natural solution for the case with easy-to-use equations as well as being widely regarded as an efficient optimization algorithm.

5.2.1 Basis on Particle Swarm Optimization

In PSO optimization is handled by a swarm $\boldsymbol{X}$ of particles $\boldsymbol{x}_{\mathrm{i}}$, each representing its individual solution within given boundaries for design variables. During the optimization process particles constantly change their design variable values in order to find the best

solution. In the model of PSO presented in "Particle swarm optimization (PSO). A tutorial" by Federico Marini and Beata Walczak [9], the change of particle values is governed by a simple formula for particle i velocity vector $\boldsymbol{v}_\mathrm{i}$, written as

$$\boldsymbol{v}_\mathrm{i}(t+1) = \boldsymbol{v}_\mathrm{i}(t) + c_1\big(\boldsymbol{p}_\mathrm{i} - \boldsymbol{x}_\mathrm{i}(t)\big)\boldsymbol{R}_1 + c_2\big(g - \boldsymbol{x}_\mathrm{i}(t)\big)\boldsymbol{R}_2 \tag{43}$$

Where sub-index i denotes particle number, t and $t+1$ indicate successive iterations, $\boldsymbol{p}_\mathrm{i}$ is personal best value for particle, $\boldsymbol{x}_\mathrm{i}$ is the set of design variables, g is the global best result found and $\boldsymbol{R}_1$, $\boldsymbol{R}_2$ are randomized values for each particle ranging 0..1. c_1 and c_2 are acceleration constants usually set within $0 \leq c_1, c_2 \leq 4$. With the calculated velocity, next particle position $\boldsymbol{x}_\mathrm{i}(t+1)$ can be determined as

$$\boldsymbol{x}_\mathrm{i}(t+1) = \boldsymbol{x}_\mathrm{i}(t) + \boldsymbol{v}_\mathrm{i}(t+1) \tag{44}$$

The process of optimization is as follows. First, swarm particles are initialized with randomized values. Second, particles $\boldsymbol{x}_\mathrm{i}$ are evaluated and they are compared with their personal best solutions $\boldsymbol{p}_\mathrm{i}$ and global best solution g, replacing values if inequality constraints, equality constraints were met and better solution was found. Third, particles are moved and the process second and third part are repeated until a stopping criterion, for example set iteration rounds, is met. At the end of the iteration process the optimization result is represented by g.

5.2.2 PSO application

For the purpose of the present study, original PSO explained in Chapter 5.2.1 was altered. Instead of calculating the personal best solution for each particle, particles are moved in a randomized direction decreasing in value towards the end of the optimization. The modification made was to increase turbulence due to the large number of design variables involved. The modified velocity vector can be described as

$$\boldsymbol{v}_\mathrm{i}(t+1) = \boldsymbol{v}_\mathrm{i}(t) + c_1\big(\boldsymbol{r}_\mathrm{i} - \boldsymbol{x}_\mathrm{i}(t)\big)\boldsymbol{R}_1 + c_2\big(g - \boldsymbol{x}_\mathrm{i}(t)\big)\boldsymbol{R}_2 \tag{45}$$

Where $\boldsymbol{r}_\mathrm{i}$ is a randomized vector of design variables within set boundaries and constant $c_1 = c - c\,\frac{iteration\ rounds\ passed}{\text{total iteration rounds}}$ and $0 \leq c \leq 4$.

The modified application of PSO has been found to work well with iterations and values of results can be found in Chapter 7.

6. PROGRAM SPECIFICATIONS

In this chapter details about program are explained. Program was written in Python 2.7 language and turned into a windows executable file (.exe) with an Open Source tool py2exe [10]. Graphical User Interface (GUI) was made with TkInter [11].

6.1 Requirements for calculation

The aim of the program is to be able to optimize a recovery boiler economizer by lowering mass while retaining heat transfer rate.

For calculation, it is possible to choose design variables, upper and lower boundaries for design variables, input values, restrictive values and desired end temperature for either gas or water. As a results, the program should yield the best geometry found by optimization loop, which then can be validated with a more accurate calculation tool. For optimization, PSO swarm size, iteration rounds and computer core amount for parallel computing can be chosen.

6.1.1 Design variables and boundary values

The design variables for the optimization can be chosen from fin width, fin thickness, pipe diameter, economizer length, economizer width, economizer depth and spacing in between elements. The geometrical attributes can be either set to a specific value Figure 11 a), or can be set to be optimized within a set range of lower and upper boundaries as shown in Figure 11 b).

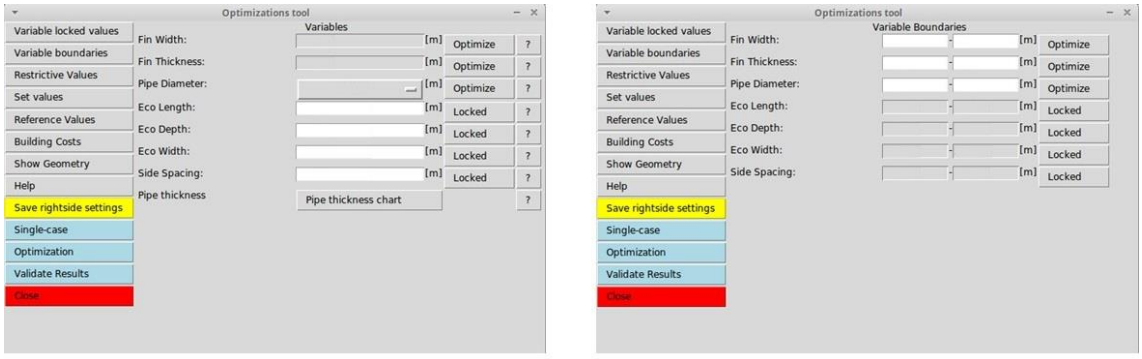

a) Choosing design variables

b) Setting boundaries

Figure 11. *Program design variable and boundary settings*

Pipe thickness is determined by chosen input value of water pressure and pipe diameter by EN-pipe standards.

6.1.2 Restrictive values

Restrictive values for calculation consist of maximum error on end temperature allowed in optimization, maximum velocity for gas in an empty economizer and maximum end temperature for outlet gas or minimum outlet temperature for water. Setting end temperature for either yields the desired heat transfer amount for the case, which can be estimated with Equation (20).

6.1.3 Input values

Input values for calculation are mass flows and inlet temperatures for gas and water, body material conduction coefficient, economizer sootblowing cavity size, design pressure for water, gas volumetric components and approximated values for fouling conduction coefficient and deposit layer thickness. Value for fouling layer thickness can be approximated by calculating a single case with an existing geometry and comparing the results to measured values from the existing geometry.

6.1.4 Results and validation

Optimization loop result geometry and heat transfer rate is saved at the end of the optimization. If a simplified model expressed in Chapter 4.7 is used for optimization, the used model will most likely yield different results than the original model. Because fouling layer thickness was approximated by using the initial heat transfer model created, the optimized result geometry has to be validated by using the original model.

6.2 Requirements for program usage

The present optimization program was intended to be a fast and easy-to-use standalone program for Microsoft Windows platform. Aside from simplifying the model, time spent for calculation can be tremendously decreased by using parallel computing, which means usage of more than processor core. For easy usage, a Graphical User Interface (GUI) is a good solution.

6.2.1 Programming language

Python 2.7 was chosen as programming language. In comparison to C++ and C languages, Python is very intuitive and easy to use. With 3rd party Open Source software py2exe[10] and Python libraries TkInter[11] and Multiprocessing, the requirements for program can be met. In addition, Python has access to useful libraries such as MatPlotLib and NumPy [12]. MatPlotLib allows generating plots out of given data, while NumPy allows usage of mathematical operations such as hyperbolic functions.

6.2.2 Graphical User Interface

Program GUI was constructed with the usage of TkInter. TkInter is a GUI Programming toolkit in Python, which offers tools for making a simple boxed GUI.

6.2.3 Parallel computing

With parallel computing the program optimization speed can be greatly increased. In parallel computing, individual tasks can be distributed to multiple processor cores. The aim of PSO in the present application is to calculate multiple geometries, which are independent from each other. The decrease of computational time can therefore be almost linearly decreased by the amount of cores used.

Parallel computing is achieved in the present program by usage of Pool-method from Python library Multiprocessing. Pool has been recorded to work well with the 3rd party conversion software py2exe.

6.3 Program calculation process

The present optimization program calculation process is as follows. First, each PSO particle is given a randomized value for the chosen design variables. Second, the heat transfer for each geometry is calculated individually. Third, all particle results are compared and best value is saved. Fourth, if set amount of iteration has not been reached, the geometries for each particle are chanced according to PSO specifications and process is repeated from the second step. If the last iteration round was reached, the best result of the optimization is saved. The optimization loop process can be expressed with a process chart shown in Figure 12.

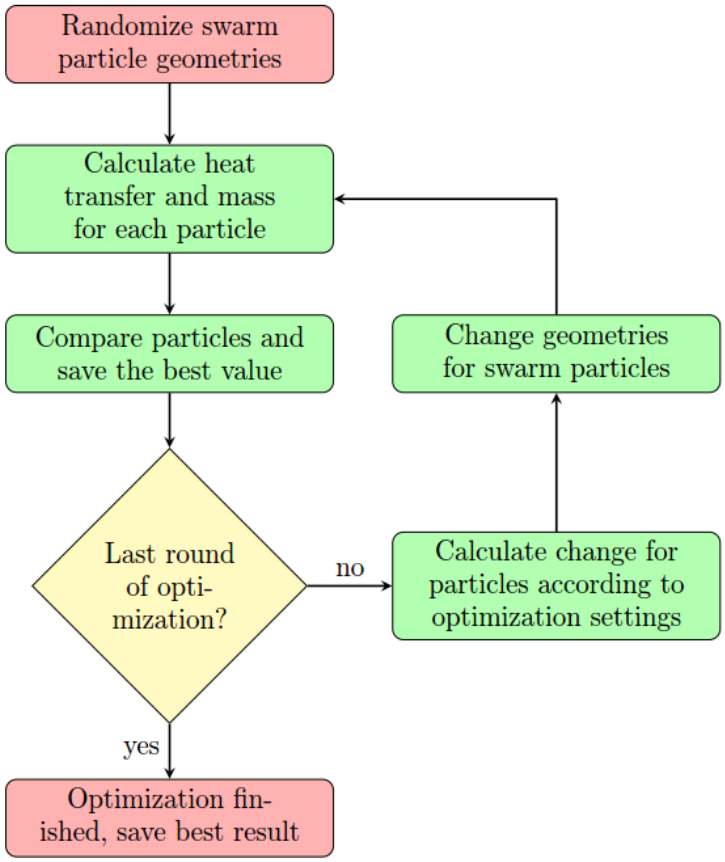

Figure 12. *Optimization process*

The process for calculation of an individual swarm particle heat transfer can be separated into smaller steps. In this calculation, the steps are as follows. First, the amount of pipes, fins and elements are calculated according to the determined values for geometry in optimization loop. Second, constant properties for fluids are initialized, initial guess for either outlet temperature is chosen and evaluation for flow characteristics is performed. Third, economizer is split into streamwise parts. Fourth, heat transfer for first part is calculated by iteration of pipe and fin intersection temperature. Fifth, gas and water temperature are changed according to length of the part and heat transfer calculated. Sixth, evaluate constant properties and flow characteristics according to the calculated temperatures. The process until step six is continued until last part of split economizer is reached. Seventh, compare the result inlet temperature value to the set inlet temperature value. In the case of incorrect value, a new outlet temperature is guessed. Otherwise, the heat transfer amount and geometry are saved for comparison with other swarm particles. This process tree can be expressed as shown in Figure 13.

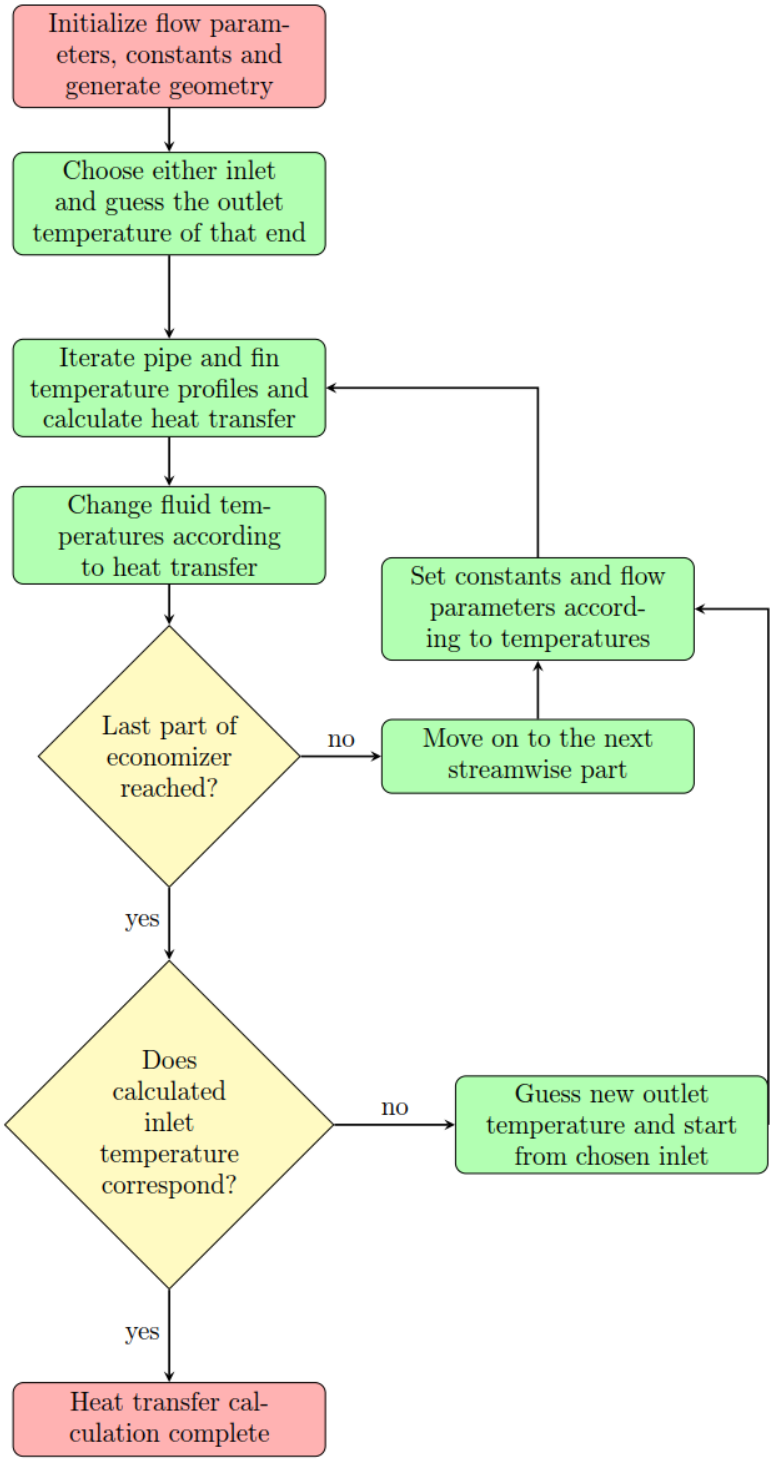

Figure 13. *Heat transfer calculation process*

In Figure 13, if a simplified model is used, it is possible to neglect intersection temperature iteration. This would speed up the process, because iteration of intersection temperature includes multiple iterations of fouling surface temperature due to particle radiation. If fluid properties were kept as constant values through the whole calculation, it could be possible to calculate the whole process with just Equation (40).

7. CALCULATION RESULTS

In this chapter results from optimization will be presented and validated. Sensitivity analysis is performed on flow properties, fluid constant values and a comparison of simplified model results to reference values is carried out.

7.1 Optimization results

Results obtained from optimization are presented here. Sample results from optimizing single variables as well as everything at once are given. Clear guidelines were found for minimizing mass in terms of heat transfer rate preservation.

Constant properties for exhaust fumes and material in use were provided by Valmet Technologies Oy. Water constant properties were evaluated with IFC-67 standard [13].

7.1.1 Full optimization

Optimizing all design variables at once gave results, in which mass can be lowered by up to $20 - 40$ % depending on boundaries set for design variables. This can be seen in figure, where mass and heat transfer are evaluated by comparison to reference values

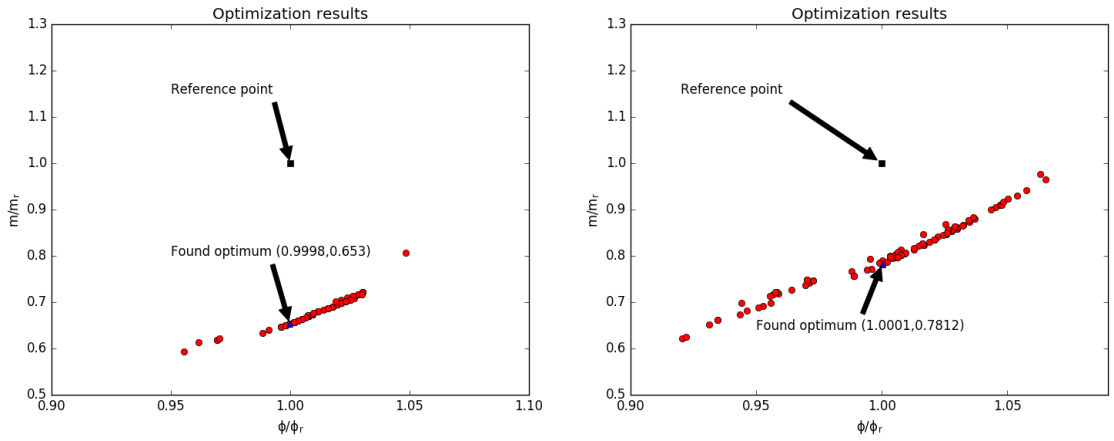

Figure 14. *Full optimization results*

Figure 14 features comparison of two optimization cases to a reference case provided by Valmet Technologies Oy. The optimization cases have different settings as boundary values. Each dot represents a single particle with individual geometrical properties, mass and heat transfer. It can be seen that heat transfer increases with higher mass and vice versa. In comparison to reference point, mass of the optimum point results as 65% in a) and 78% in b) of the reference value with the same heat transfer amount.

7.1.2 Optimizing single design variables

After obtaining results with a clear decrease in mass while preserving heat transfer rate, interests lie in how single geometrical dimensions were changed in order to obtain the results. During multiple optimizations, guidelines for changing individual design variables were found. Most clear results were found when optimization was directed at fin thickness, pipe diameter and spacing in between the elements.

Fin thickness

Change in fin thickness has a linear effect to economizer weight and only a little effect towards other design variables. Therefore, it is easy to make an observation of fin thickness effect on heat transfer rate. Two different setups for economizers geometrical variables were used to determine fin thickness effect on heat transfer rate as shown in Figure 15

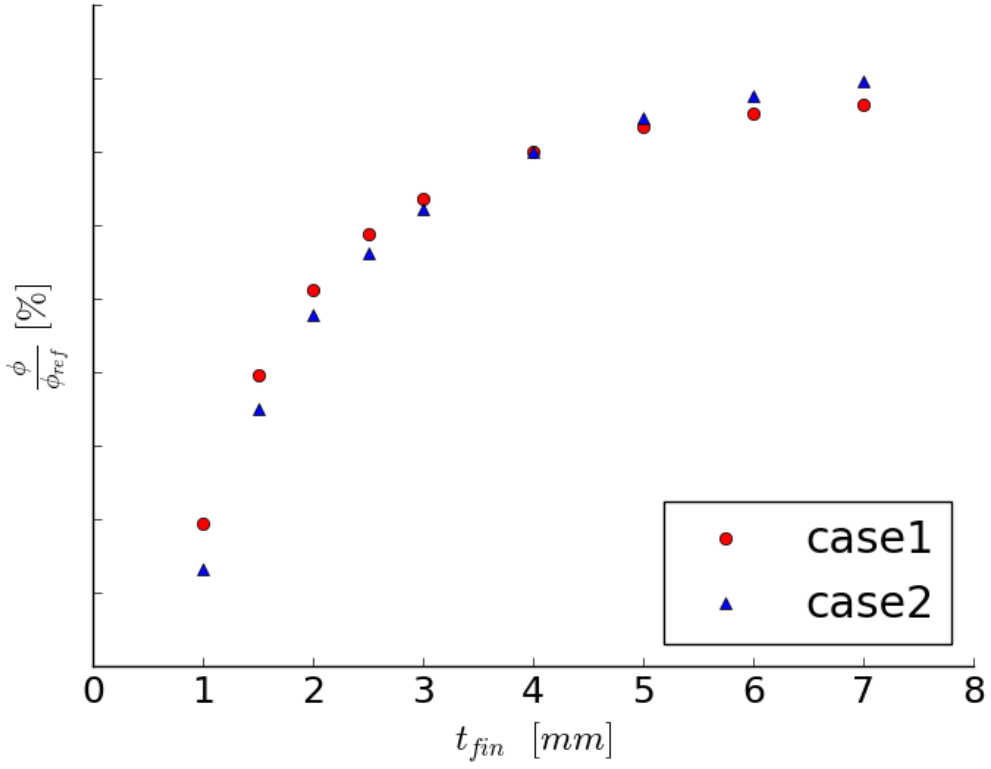

Figure 15. *Heat transfer by fin thickness*

In both cases of Figure 15, design variables apart from fin thickness were kept constant. The vertical axis values are linearly distributed. Calculated heat transfer at thickness of 4 mm was used as reference value for heat transfer rate. Effect of fin thickness change can be deducted from gradient of heat transfer rate change by fin thickness change which, for the two cases, is highest from one to three millimeters and lower from four millimeters onwards.

Pipe diameter

Optimization of pipe diameter values can be expressed by comparing heat transfer per pipe mass for a meter of pipe $\frac{\phi}{m}$. Results for comparing these values is shown in Figure 16.

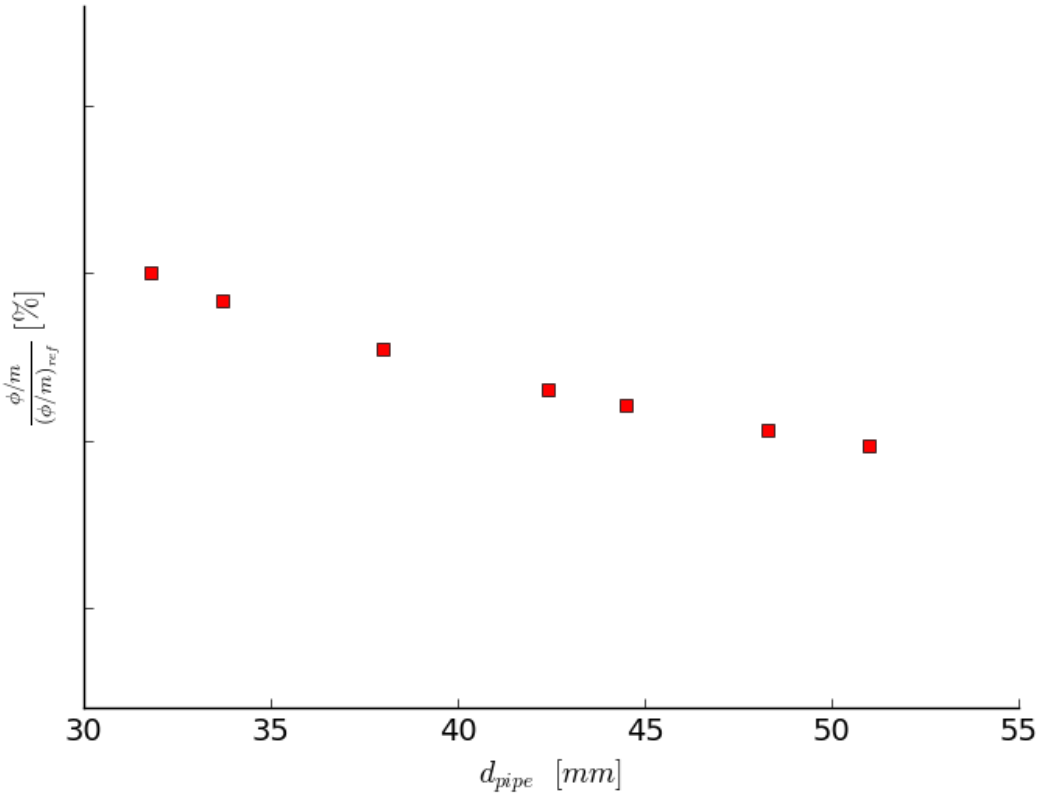

Figure 16. *Heat transfer per kilogram of pipe, pipe thickness 4 mm*

Values for reference point was calculated at pipe diameter 31.8 mm. Heat transfer per pipe kilogram decreases when pipe diameter is increased. Values for pipe diameter in Figure 16 are EN-pipe standards calculated with wall thickness of 4 mm.

Element spacing

Element spacing effect to heat transfer in terms of heat transfer is easy to estimate, since it doesn't have effect on economizer mass as long as economizer width is changed with it. Flow channel dimensions have an impact on pressure drop, which is why it is important to include pressure loss by friction calculated with Equation (14) to results. Table 1 includes estimation percentage-wise pressure drop change to reference geometry when element spacing is altered, as well as estimation of impact on heat transfer and flow velocity.

Table 1. *Element spacing effect on heat transfer and pressure loss*

$d_{\text{elements}}\ [mm]$	$\frac{\phi-\phi_{\text{ref}}}{\phi_{\text{ref}}}\ [\%]$	$\frac{\Delta p_{\text{fric}}-\Delta p_{\text{ref,fric}}}{\Delta p_{\text{ref,fric}}}\ [\%]$	$\frac{V-V_{\text{ref}}}{V_{\text{ref}}}\ [\%]$
115	+0 %	+0 %	+0 %
105	+1 %	+36 %	+9 %
90	+3 %	+133 %	+27 %
80	+5 %	+256 %	+39 %
70	+7 %	+486 %	+58 %
60	+8 %	+964 %	+88 %

In Table 1, calculation geometry with 115 millimeters as element spacing was used as reference point. While mass was kept constant, it is clear that when reducing the element spacing, the pressure drop increases at huge rate while heat transfer rate change is minimal in comparison. For calculation of friction factor, surface roughness of $0{,}05 * 10^{-3}\ mm$ was used, which is equal to surface roughness of carbon steel.

7.2 Gas pressure drop evaluation

In terms of design variables, gas pressure drop by friction is dependent on the length of the economizer and hydraulic diameter of the pipe-fin -element. Table 1 shows a good relation of element spacing effect on friction loss by pressure. Gas pressure drop by friction can be evaluated from reference pressure drop by Equations (17) and (18).

As mentioned in Chapter 3.3, minor losses are troublesome to calculate due to complex inflow configuration. Due to the lack of reliable calculation method for pressure loss calculation by minor losses, the calculation is omitted.

7.3 Sensitivity analysis

Sensitivity analysis was carried out on effect of changing constant properties, fluid characteristics and the usage of a simplified model for calculation.

7.3.1 Evaluation of Constant properties

The constant properties needed for calculation are viscosity v, density ρ, specific heat capacity c_p and Prandtl number Pr, which may be calculated with thermal diffusivity α

as stated with Equation (9). Gas constant properties are evaluated as dry air at atmospheric pressure for different temperatures and water properties are evaluated with IFC-67 standard by pressure of 100 bars and changing temperature.

Appendix A is a table of dry air constant properties, of which we can see, that Prandtl number Pr and specific heat capacity c_p remain relatively constant for gas in range 100-600 degrees Celsius. Density ρ and kinematic viscosity v have a larger change and thus their effect on overall heat transfer rate must be evaluated with the program. Below is a table of two different cases, where a reference case is being compared to same geometry while using uniform values of density and viscosity at reference temperature $T_{ref} = \frac{T_{in}+T_{out}}{2}$.

Table 2. *Gas constant change effect on heat transfer rate*

	$\frac{\phi - \phi_{\mathrm{ref}_1}}{\phi_{\mathrm{ref}_1}} * 100\%$	$\frac{\phi - \phi_{\mathrm{ref}_2}}{\phi_{\mathrm{ref}_2}} * 100\%$
Uniform ρ_{gas}	$-0{,}02\ \%$	$-0{,}01\ \%$
Uniform ν_{gas}	$-2{,}23\ \%$	$-6{,}88\ \%$

From Table 2 it can be seen that density change of flue gas does not affect end heat transfer rate. Viscosity change on the other hand has a much bigger effect, because it directly affects convection coefficient of gas h_g through Reynolds number Re_D, which is used in heat transfer calculation.

Appendix B shows a table of water properties from 100 to 300 degrees Celsius at 100 bar pressure. It can be seen that the water constant properties are changing with temperature, which shows that they should be studied.

Table 3. *Water constant change effect on heat transfer rate*

	$\frac{\phi - \phi_{\mathrm{ref}_1}}{\phi_{\mathrm{ref}_1}} * 100\%$	$\frac{\phi - \phi_{\mathrm{ref}_2}}{\phi_{\mathrm{ref}_2}} * 100\%$
Uniform ρ_{water}	$+0.01\%$	$+0.03\ \%$
Uniform ν_{water}	$+0.01\ \%$	$+0.02\ \%$
Uniform $c_{p_{\mathrm{water}}}$	$+0{,}31\ \%$	$+0.26\ \%$

From Table 3 it can be seen, that water constant properties can be estimated as of constant value, because changing them has little to no effect at all on heat transfer.

7.3.2 Evaluation of Fluid Characteristics

Evaluation on which of the flow characteristics are important is an interesting topic to tackle. The characteristics in question include Reynolds number, convection coefficient, flow speed and emissivity of gas. Table 4 includes calculated effect on keeping each of the characteristics constant in calculation. The comparison was tested with two reference cases and presented as a percentage difference from the reference case with equation $\frac{\phi-\phi_{\mathrm{ref}}}{\phi_{\mathrm{ref}}} * 100\%$.

Table 4. *Uniform flow property evaluation on heat transfer rate*

	$\frac{\phi-\phi_{\mathrm{ref}_1}}{\phi_{\mathrm{ref}_1}} * 100\%$	$\frac{\phi-\phi_{\mathrm{ref}_2}}{\phi_{\mathrm{ref}_2}} * 100\%$
Uniform h_{water}	-0.03%	-1.17%
Uniform Re_{water}	-0.12%	-1.13%
Uniform V_{water}	-1.13%	-1.13%
Uniform h_{gas}	-0.10%	-1.05%
Uniform Re_{gas}	-1.59%	-2.79%
Uniform V_{gas}	$+5.63\%$	$+4.41\%$
Emissivity $\epsilon = 0.0$	-6.81%	-4.0%
Emissivity $\epsilon = 0.1$	-4.13%	-2.5%
Emissivity $\epsilon = 0.2$	-1.9%	-1.18%

From Table 4 it can be seen that the most important characteristic are from gas side. Reynolds number Re_{gas}, velocity Constant V_{gas} and emissivity ϵ have the biggest impact on results and by comparing of the two cases, the impact changes when geometry is altered. Water flow properties on the other hand do not have that big effect on the end result.

7.3.3 Simplified model comparison to original model

The most time-consuming parts in the optimization are iterations of intersection points in between pipe fin and fin. These iterations include numerous of iterations over fouling layer surface temperature and are done in every single element calculation. Table 5 shows the comparison of two reference cases computed with initial model to two simplified models. Simplified model 1 includes an estimation of uniform temperature profile over pipe of water temperature value. Simplified model 2 also assumes pipe temperature as water temperature and additionally neglects radiation.

Table 5. *Comparison of simplified models to reference model*

	Reference 1 $\frac{\phi-\phi_{\mathrm{ref}}}{\phi_{\mathrm{ref}}} * 100\%$	Reference 1 $\frac{t-t_{\mathrm{ref}}}{t_{\mathrm{ref}}} * 100\%$	Reference 2 $\frac{\phi-\phi_{\mathrm{ref}}}{\phi_{\mathrm{ref}}} * 100\%$	Reference 2 $\frac{t-t_{\mathrm{ref}}}{t_{\mathrm{ref}}} * 100\%$
Simplified model 1	$+3.72\ \%$	$-78.22\ \%$	$+1.09\ \%$	$-77.55\ \%$
Simplified model 2	$-1.71\ \%$	$-83.89\ \%$	$-0.87\ \%$	$-82.18\ \%$

From Table 5 it can be seen that decrease in calculation time $\frac{t-t_{\mathrm{ref}}}{t_{\mathrm{ref}}}$ is drastic while heat transfer rate difference to original model $\frac{\phi-\phi_{\mathrm{ref}}}{\phi_{\mathrm{ref}}}$ is very minimal. Simplified model 2 is actually closer to reference value, because uniform temperature at pipe surface increases heat transfer while neglecting radiation reduces heat transfer.

After gaining information that over 80 % of calculation time can be suppressed by simplifications of the model with minimal difference to heat transfer rate, it should clear that optimization process should be carried out with either of the two simplified models instead of the original model. Further investigation on how many parts the economizer should be split in might also reduce needed calculation time by a large amount.

8. DISCUSSION OF RESULTS

In this chapter, results obtained for Chapter 7 are being discussed, as well as future improvements for the case.

8.1 Optimization achievements

As shown in Figure 14, it is possible to optimize the current economizers in use to a large extent. In particular, individual design parameters were found to have a general direction in optimization. Pipe diameter is to be minimized, fin thickness optimal value is on the lower end and element spacing should be kept at reasonable values due to pressure loss by friction. Moreover, element spacing affects overall deposit layer generated by flue gas, which has to be approximated by experimental results.

The original generated model could be optimized in calculation speed by 75 % by assuming pipe to have a uniform temperature value of water. Further simplifications resulted in calculation reduction by up to 82 %. Constant properties at a reference temperature value simplify the case even further.

8.2 Further possibilities

Optimal economizer geometry when all parameters were optimized could be achieved within few hours with even a slower computer. Simplified design offered a vast increase in computation speed and with alteration to how many parts economizer should be split in; the process could be sped up even more. Additionally, the amount of needed iteration rounds could be optimized by the program itself by comparing the results found in previous optimizations.

Mechanical constraints such as thermal stresses and whether a certain configuration can be built was not featured in any way within the model. Applying these constraints would filter out any unwanted results.

Moreover, the initial geometry of the economizer was not optimized in any way. A research should be carried out where pipes had fins attached in economizer width-direction as well. Additionally, if the counter-flow setup could be changed to a cross-flow design, it would be possible to gain even more in terms of weight loss. Body material of the economizer should affect fouling as well by how well the fouling sticks to the material. This could be lessened by coating the material or by changing the material to something else.

REFERENCES

[1] Giampietro Fabbri, Heat transfer optimization in internally finned tubes under laminar flow conditions, Int. J. Heat Mass Transfer Vol. 41, No. 10, pp. 1243-1253, 1998

[2] R. Karvinen, T. Karvinen, Optimum Geometry of Plate Fins, Journal of Heat Transfer, Aug 2012, Vol.134.

[3] King-Leung Wong, Ming-Tsun Ke, Shi-Shi Ku, "The log mean heat transfer rate method of heat exchanger considering the influence of heat radiation", Energy Conversion and Management, vol 50, pp. 2693–2698, 2009

[4] E. Vakkilainen, J. Pöyry, Development of recovery boiler technology, 2003

[5] Mills A. F., Basic Mass Heat & Mass Transfer 2^{nd} edition, Prentice Hall, 1999

[6] Colebrook, C. F.; White, C. M. (1937). "Experiments with Fluid Friction in Roughened Pipes". Proceedings of the Royal Society of London. Series A, Mathematical and Physical Sciences. 161 (906): 367–381.

[7] R. Karvinen, Lämpötekniikan perusteet osa II, Tampereen Teknillinen Yliopisto, 2015

[8] Martins, J. R. R. A. and Lambe, A. B., "Multidisciplinary design optimization: A Survey of architectures", AIAA Journal, 51(9), 2013

[9] Federico Marini, Beata Walczak, Particle swarm optimization (PSO). A tutorial, Chemometrics and Intelligent Laboratory Systems, Volume 149, Part B, 15 December 2015, Pages 153–165

[10] py2exe, 25.7.2016, http://www.py2exe.org/

[11] TkInter, 25.7.2016, https://docs.python.org/2/library/tkinter.html

[12] NumPy, 25.7.2016, http://www.numpy.org/

[13] VDI-Wasserdampftafeln 7.Aufl, VDI Steam Tables 7th Edition

APPENDIX A: Physical properties of dry air at atmospheric pressure

T [°C]	$\rho \left[\frac{\text{kg}}{\text{m}^3}\right]$	$v \left[\frac{m^2}{s}\right] * 10^6$	$c_p \left[\frac{kJ}{kgK}\right]$	Pr
100	0,946	23,13	1,009	0,688
150	0,83	28,94	1,014	0,683
200	0,746	34,85	1,026	0,680
250	0,674	40,61	1,038	0,677
300	0,615	48,33	1,047	0,674
350	0,566	55,46	1,059	0,676
400	0,524	63,09	1,088	0,678
450	0,490	71,64	1,091	0,682
500	0,456	79,38	1,093	0,687
550	0,430	88,14	1,103	0,696
600	0,404	96,89	1,114	0,699

APPENDIX B: PROPERTIES OF WATER AT 100 BAR

T [°C]	$\rho \left[\frac{\text{kg}}{\text{m}^3}\right]$	$v \left[\frac{m^2}{s}\right] * 10^6$	$c_p \left[\frac{kJ}{kgK}\right]$	Pr
100	962,93	0,3	4,19	1,78
150	922,32	0,2	4,28	1,16
200	870.95	0,16	4,45	0,92
250	805,7	0,13	4,79	0,80
300	715,29	0,12	5,68	0,89